

# Detecting Chiral Orbital Angular Momentum by Circular Dichroism ARPES

Jin-Hong Park,<sup>1</sup> Choong H. Kim,<sup>2</sup> Jun Won Rhim,<sup>3</sup> and Jung Hoon Han<sup>1,\*</sup>

<sup>1</sup>*Department of Physics and BK21 Physics Research Division,  
Sungkyunkwan University, Suwon 440-746, Korea*

<sup>2</sup>*Department of Physics and Astronomy, Seoul National University, Seoul 151-742, Korea*

<sup>3</sup>*School of Physics, Korea Institute for Advanced Study, Seoul 130-722, Korea*

(Dated: November 6, 2018)

We show, by way of tight-binding and first-principles calculations, that a one-to-one correspondence between electron's crystal momentum  $\mathbf{k}$  and non-zero orbital angular momentum (OAM) is a generic feature of surface bands. The OAM forms a chiral structure in momentum space much as its spin counterpart in Rashba model does, as a consequence of the inherent inversion symmetry breaking at the surface but not of spin-orbit interaction. Circular dichroism (CD) angle-resolved photoemission (ARPES) experiment is an efficient way to detect this new order, and we derive formulas explicitly relating the CD-ARPES signal to the existence of OAM in the band structure. The cases of degenerate  $p$ - and  $d$ -orbital bands are considered.

PACS numbers:

Electron spins are quenched in ordinary crystalline solids in the sense that each crystal momentum  $\mathbf{k}$  comes in degenerate pairs of spin-up and spin-down electrons. Such degeneracy is lifted in an interesting manner for the so-called Rashba system[1], in which the given momentum state in the band has only one spin state associated with it. Examples of Rashba-split bands are many by now[2]. On symmetry grounds, as Rashba originally argued, the inherent inversion symmetry breaking (ISB) at the surface termination allows an interaction term, the Rashba term, of the form  $H_R = \lambda_R \hat{z} \cdot (\mathbf{k} \times \boldsymbol{\sigma})$  involving the coupling of the electron's spin operator  $\boldsymbol{\sigma}/2$  and its momentum  $\mathbf{k}$  (We set  $\hbar \equiv 1$ ). The chiral spin angular momentum (SAM) structure in momentum space follows as a direct consequence of the Rashba Hamiltonian  $H_R$ [3, 4].

One must note, however, that other physical quantities having the character of angular momentum can take the place of  $\boldsymbol{\sigma}$  in the Rashba Hamiltonian. For instance, in bands where the orbital angular momentum (OAM) remains unquenched, one can equally well consider a coupling of  $\mathbf{k}$  to OAM operator,  $\mathbf{L}$ . In this paper, we expand this observation to show that chiral OAM in one-to-one correspondence with the electron's linear momentum is indeed a general consequence of ISB for the surface bands. Unlike the chiral SAM structure which typically occurs in materials with strong spin-orbit interaction (SOI)[2], we show that chiral OAM occurs even for materials with no SOI.

We begin by providing a simple, tight-binding (TB) model Hamiltonian in two dimensions where the above-mentioned chiral OAM structure emerges. A three-fold degenerate  $p$ -orbital system is considered, while the spin degrees of freedom is suppressed in order to emphasize the notion of chiral OAM emerging from ISB alone without the requirement of SOI. The TB model is the triangular lattice version of the square one originally considered

by Petersen and Hedegård[5] in their study of Rashba phenomena in  $p$ -orbital bands. By suppressing spin degrees of freedom, we do away with the notion of conventional Rashba spin splitting. The idea of ISB-induced chiral OAM was not considered in Ref. 5 or in any other literature we are aware of[6].

We introduce two Slater-Koster parameters  $V_1$  and  $V_2$  for  $\sigma$ - and  $\pi$ -bonding amplitudes, respectively, and a third one,  $\gamma$ , representing the degree of ISB[5]. We will write  $N$  for the number of sites in the lattice, and  $|i, \lambda\rangle$  for the localized Wannier orbitals ( $\lambda = p_x, p_y, p_z$ ) at the atomic site  $\mathbf{r}_i$ . Then the tight-binding Hamiltonian for the triangular lattice (essentially the same result obtains for square lattice) near the  $\Gamma$ -point ( $\mathbf{k} = 0$ ) in the momentum-space basis  $|\mathbf{k}, \lambda\rangle = N^{-1/2} \sum_i e^{i\mathbf{k}\cdot\mathbf{r}_i} |i, \lambda\rangle$  becomes

$$H_{\mathbf{k}} = \begin{pmatrix} \alpha k_x^2 + \beta k_y^2 & (\alpha - \beta)k_x k_y & -i\frac{3}{2}\gamma k_x \\ (\alpha - \beta)k_x k_y & \alpha k_y^2 + \beta k_x^2 & -i\frac{3}{2}\gamma k_y \\ i\frac{3}{2}\gamma k_x & i\frac{3}{2}\gamma k_y & 4(\alpha - \beta) - \frac{3}{2}V_2 k^2 \end{pmatrix}. \quad (1)$$

Here,  $\alpha = 3(3V_1 - V_2)/8$ ,  $\beta = 3(V_1 - 3V_2)/8$  and  $k^2 = k_x^2 + k_y^2$ . The lattice constant is taken to be unity. To diagonalize  $H_{\mathbf{k}}$ , it is convenient to choose a new set of basis vectors

$$\begin{aligned} |\mathbf{k}, \text{I}\rangle &= (k_y/k)|\mathbf{k}, p_x\rangle - (k_x/k)|\mathbf{k}, p_y\rangle, \\ |\mathbf{k}, \text{II}\rangle &= (k_x/k)|\mathbf{k}, p_x\rangle + (k_y/k)|\mathbf{k}, p_y\rangle, \\ |\mathbf{k}, \text{III}\rangle &= e^{-i\phi_{\mathbf{k}}}|\mathbf{k}, p_z\rangle, \end{aligned} \quad (2)$$

$k = |\mathbf{k}|$ ,  $e^{i\phi_{\mathbf{k}}} = (k_x + ik_y)/k$ . The state  $|\mathbf{k}, \text{I}\rangle$  remains decoupled at energy  $E_{1,\mathbf{k}} = 3V_2 - 3V_1 + 3(V_1 - 3V_2)\mathbf{k}^2/8$ , while  $|\mathbf{k}, \text{II}\rangle$  and  $|\mathbf{k}, \text{III}\rangle$  combine to form eigenstates which, to leading order of  $\gamma/\Delta$ , are

$$\begin{aligned}
|\mathbf{k}, 2\rangle &\simeq |\mathbf{k}, \text{II}\rangle - \frac{i\gamma(k_x - ik_y)}{2\Delta} |\mathbf{k}, \text{III}\rangle, \\
|\mathbf{k}, 3\rangle &\simeq |\mathbf{k}, \text{III}\rangle - \frac{i\gamma(k_x + ik_y)}{2\Delta} |\mathbf{k}, \text{II}\rangle,
\end{aligned} \quad (3)$$

with energies  $E_{2,\mathbf{k}} \simeq 3(V_2 - V_1) + 3((3V_1 - V_2)/8 - \gamma^2/4\Delta)\mathbf{k}^2$  and  $E_{3,\mathbf{k}} \simeq 6V_2 + (3\gamma^2/4\Delta - 3V_2/2)\mathbf{k}^2$ . The OAM operator is given by the sum  $\mathbf{L} = (1/N)\sum_i \mathbf{L}_i$  where each  $\mathbf{L}_i$  acts on the Wannier state  $|i, \lambda\rangle$  as the usual  $L = 1$  angular momentum operator. The two bands obtained above carry nonzero, chiral OAM as claimed ( $L^+ = L^x + iL^y$ ):

$$\langle \mathbf{k}, 2 | L^+ | \mathbf{k}, 2 \rangle = \frac{i\gamma}{\Delta} (k_x + ik_y) = -\langle \mathbf{k}, 3 | L^+ | \mathbf{k}, 3 \rangle. \quad (4)$$

The ‘‘helicities’’ of the chiral OAMs are opposite between the bands, with their magnitudes vanish linearly with  $|\mathbf{k}|$  and the ISB parameter  $\gamma$ . In contrast the Rashba model displays perfect spin polarization irrespective of the wave vector or the strength of the Rashba parameter  $\lambda_R$ .

A second check on the existence of chiral OAM is performed by employing the first-principles local-density approximation (LDA) calculation for a Bi single layer forming a triangular lattice. The choice is inspired by Bi being a proto-typical  $p$ -orbital band material. An external electric field of  $3\text{V}/\text{\AA}$  perpendicular to the layer was imposed by hand to mimic the surface potential gradient without having the complication of dealing with the bulk states. We also performed calculations for the physically more realistic case of Bi bi-layer with perpendicular electric field[8], with results that are entirely in accord with the statements made below for the single-layer case regarding the emergence of chiral OAM. To emphasize the relevance of ISB we again chose to investigate the spin-degenerate case by turning off SOI in the LDA calculation. The resulting electronic structure for spinless case consisting of three  $p$ -orbital-derived bands is shown in Fig. 1(a). As the external electric field is turned on, a level repulsion between the middle ( $E_2$  in Fig. 1(a)) and the bottom ( $E_3$  in Fig. 1(a)) band occurs as indicated by circles in Fig. 1(a). These two bands exhibit the chiral OAM patterns with the maximum OAM vector  $|\langle \mathbf{L} \rangle| \approx 0.96\hbar$  as shown in Fig. 1(c) and 1(d), while the third one, shown in Fig. 1(b), carries much less OAM around the  $\Gamma$  point. The OAM chiralities of the two bands are opposite, in accordance with the previous TB analysis. An excellent fit of the LDA band structure near the  $\Gamma$  point was possible with the TB parameters  $V_1 = -0.725$  eV,  $V_2 = -0.11$  eV and  $\gamma = 0.2623$  eV (Fig. 1(a)). The OAM magnitude is seen to decrease continuously upon approaching the  $\Gamma$  point in the LDA calculation (Fig. 1(c) and 1(d)) as predicted by the TB calculation, Eq. (4).

Having established theoretically the existence of chiral OAM in generic inversion-asymmetric bands by a

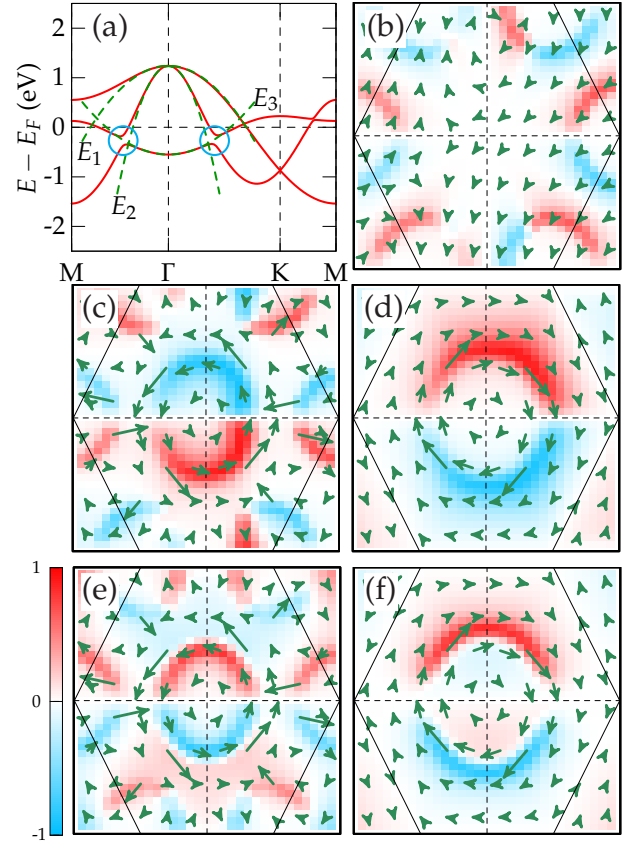


FIG. 1: OAM and CD from first-principles and tight-binding calculations of Bi monolayer without SOI. (a) LDA band structure for Bi monolayer with SOI turned off. Perpendicular electric field of  $3\text{V}/\text{\AA}$  was imposed externally. Three dashed curves represent the tight-binding energy dispersions around the  $\Gamma$  point. (b)-(d) OAM vectors (green arrows) and NCD signals (color backgrounds) for the three bands,  $E_1$ (b),  $E_2$ (c), and  $E_3$ (d) over the whole Brillouin zone marked by a solid hexagon. Largest OAM has magnitude  $\approx 1\hbar$  for bands  $E_2$  and  $E_3$ . NCD is calculated with  $k_{F,z} = 2.27\text{\AA}^{-1}$ . (e)-(f) NCD calculated with  $k_{F,z} = 0$  in Eq. (12) for  $E_2$ (e) and  $E_3$ (f) bands. The opposite color assignments between (c) and (e) is a consequence of photon energy dependence of the scattering intensity.

number of methods, we turn to the question of its detection. Spin- and angle-resolved photoemission spectroscopy (SARPES) has served to identify the chiral spin structure of the surface bands in the past[3, 4]. A similar chiral structure for OAM as demonstrated here cannot, however, be detected by the same probe since chiral OAM exists even when SOI is very weak and spin degeneracy is nearly perfect. Given the potential prevalence of chiral OAM in ordinary, *i.e.* weak SOI, surface bands, it is essential to establish detection tools for this new degree of freedom in band materials and develop some theory of it.

Circular dichroism (CD) refers to phenomena in which the physical response of a system to probing light de-

pends systematically on the light polarization being left-circularly-polarized (LCP) or right-circularly-polarized (RCP). In ARPES, CD manifests itself as different scattering intensities of the photo-electrons depending on the helicity of incident light being RCP or LCP. The CD-ARPES signal can be quantified through the normalized CD (NCD) defined as

$$D(\mathbf{k}) = \frac{\sum_{\sigma} (I_{\sigma}^{\text{RCP}}(\mathbf{k}) - I_{\sigma}^{\text{LCP}}(\mathbf{k}))}{\sum_{\sigma} (I_{\sigma}^{\text{RCP}}(\mathbf{k}) + I_{\sigma}^{\text{LCP}}(\mathbf{k}))}. \quad (5)$$

The sum over the final state spin  $\sigma$  reflects the spin-integrated nature of the detection scheme. Spin index is restored in the following derivation of the NCD formula as it will apply equally well to strong-SOI materials with mixed spins.

The initial state  $|I\rangle$  is the Bloch state of momentum  $\mathbf{k}$  constructed as  $|\mathbf{k}, \mathbf{m}\rangle = N^{-1/2} \sum_i e^{i\mathbf{k}\cdot\mathbf{r}_i} |i, \mathbf{m}\rangle$ . The Wannier state  $|i, \mathbf{m}\rangle$  at site  $\mathbf{r}_i$  is given by

$$|i, \mathbf{m}\rangle = \sum_{\lambda, \sigma} m_{\lambda, \sigma}(\mathbf{k}) |i, \lambda, \sigma\rangle, \quad (6)$$

as a linear combination of constituent atomic orbitals labeled by  $\lambda$ , and spin  $\sigma$ , with  $\mathbf{k}$ -dependent coefficients  $m_{\lambda, \sigma}(\mathbf{k})$ . Usual plane wave forms are assumed for the final state:  $\psi_F \sim e^{i\mathbf{k}_F \cdot \mathbf{r}}$ .

The transition amplitude into the final state of spin  $\sigma$  is evaluated as

$$\begin{aligned} \langle F, \sigma | \mathbf{p} \cdot \mathbf{A} | I \rangle &\sim \langle F, \sigma | \mathbf{r} \cdot \mathbf{A} | I \rangle \\ &\sim \sum_{i, \lambda} m_{\lambda, \sigma}(\mathbf{k}) \langle F | \mathbf{r} \cdot \mathbf{A} | i, \lambda \rangle e^{i\mathbf{k}\cdot\mathbf{r}_i}. \end{aligned} \quad (7)$$

Given the localized nature of the Wannier state, it is useful to re-write  $\mathbf{r} \cdot \mathbf{A} = (\mathbf{r} - \mathbf{r}_i) \cdot \mathbf{A} + \mathbf{r}_i \cdot \mathbf{A}$ . One immediately finds that  $\langle F | \mathbf{r}_i \cdot \mathbf{A} | I \rangle = (\mathbf{r}_i \cdot \mathbf{A}) \langle F | I \rangle$  is zero from the presumed orthogonality of the initial and the final states. To proceed further, we treat the cases of  $p$ -orbital and  $d$ -orbital bands separately as they require somewhat different strategies for evaluation of the NCD formula. For  $p$ -orbitals the Wannier states are assigned the hydrogenic wave function  $\langle i | \lambda \rangle \sim (\mathbf{r} - \mathbf{r}_i)_{\lambda} f(|\mathbf{r} - \mathbf{r}_i|)$  ( $\lambda = x, y, z$ ) and with these we find the transition amplitude becomes

$$\begin{aligned} &\sum_i e^{i(\mathbf{k} - \mathbf{k}_F) \cdot \mathbf{r}_i} \left( \sum_{\lambda} m_{\lambda, \sigma}(\mathbf{k}) \int e^{-i\mathbf{k}_F \cdot \mathbf{r}} [\mathbf{r} \cdot \mathbf{A}] x_{\lambda} f(|\mathbf{r}|) \right) \\ &\propto \sum_{\lambda} m_{\lambda, \sigma}(\mathbf{k}) \int e^{-i\mathbf{k}_F \cdot \mathbf{r}} [\mathbf{r} \cdot \mathbf{A}] x_{\lambda} f(|\mathbf{r}|). \end{aligned} \quad (8)$$

The sum  $\sum_i e^{i(\mathbf{k} - \mathbf{k}_F) \cdot \mathbf{r}_i} = \delta(\mathbf{k}_F^{\parallel} - \mathbf{k} + \mathbf{G})$  simply yields in-plane momentum conservation up to the reciprocal lattice

vector  $\mathbf{G}$ . Making use of the fact that  $f(|\mathbf{r}|)$  depends only on the radial distance, one can re-write the second line of Eq. (8) as

$$-A_{\alpha} m_{\beta, \sigma} \partial_{\alpha} \partial_{\beta} \int e^{-i\mathbf{k}_F \cdot \mathbf{r}} f(|\mathbf{r}|) d^3 \mathbf{r} = -\mathbf{A} \cdot \nabla_{\mathbf{k}_F} g_{\sigma}(\mathbf{k}_F), \quad (9)$$

where we have introduced

$$\begin{aligned} f(|\mathbf{k}_F|) &= \int e^{-i\mathbf{k}_F \cdot \mathbf{r}} f(|\mathbf{r}|) d^3 \mathbf{r}, \\ g_{\sigma}(\mathbf{k}_F) &= \mathbf{m}_{\sigma} \cdot \nabla_{\mathbf{k}_F} f(|\mathbf{k}_F|), \end{aligned} \quad (10)$$

and  $\mathbf{m}_{\sigma} = (m_{x, \sigma}, m_{y, \sigma}, m_{z, \sigma})$ . One finds the average OAM  $\langle \mathbf{L} \rangle$  for the  $p$ -orbital Bloch states  $|\mathbf{k}, \mathbf{m}\rangle$  expressed simply in terms of  $\mathbf{m}_{\sigma}$ :

$$\langle \mathbf{k}, \mathbf{m} | \mathbf{L} | \mathbf{k}, \mathbf{m} \rangle \equiv \langle \mathbf{L} \rangle = i \sum_{\sigma} \mathbf{m}_{\sigma}(\mathbf{k}) \times \mathbf{m}_{\sigma}^*(\mathbf{k}). \quad (11)$$

Of great importance is the fact that nonzero OAM is possible even with spin degeneracy,  $\mathbf{m}_{\sigma} = \mathbf{m}$ , where one would obtain  $\langle \mathbf{L} \rangle = 2i\mathbf{m} \times \mathbf{m}^*$ . We can now proceed to show that NCD is fundamentally related to  $\langle \mathbf{L} \rangle$ . Equations (8) and (10) allow the NCD formula (5) to be re-cast in the compact, suggestive form:

$$D(\mathbf{k}) = \frac{(\mathbf{A} \times \mathbf{A}^*) \cdot \sum_{\sigma} \nabla g_{\sigma} \times \nabla g_{\sigma}^*}{\sum_{\sigma} [(\mathbf{A} \cdot \nabla g_{\sigma})(\mathbf{A}^* \cdot \nabla g_{\sigma}^*) + (\mathbf{A}^* \cdot \nabla g_{\sigma})(\mathbf{A} \cdot \nabla g_{\sigma}^*)]} \quad (12)$$

Explicit reference to  $\mathbf{k}_F$  in the derivatives has been dropped from above. The vector potentials are  $\mathbf{A} = (\varepsilon_1 + i\varepsilon_2)/\sqrt{2}$  for RCP and  $\mathbf{A}^*$  for LCP, with  $\mathbf{A} \times \mathbf{A}^* = -i\varepsilon_1 \times \varepsilon_2 = -i\hat{k}_{\text{ph}}$  giving the photon direction. The remaining task is to evaluate the quantity  $\sum_{\sigma} \nabla g_{\sigma} \times \nabla g_{\sigma}^*$  which governs the CD response of the given initial state. The denominator, by definition, is always positive and plays a minor role in characterizing the OAM structure.

For  $p$ -orbitals, inserting  $g_{\sigma} = \mathbf{m}_{\sigma} \cdot \nabla f$  gives

$$\begin{aligned} \sum_{\sigma} \nabla g_{\sigma} \times \nabla g_{\sigma}^* &= \frac{1}{2} \varepsilon^{\alpha\beta\gamma} (\mathbf{m}_{\sigma} \times \mathbf{m}_{\sigma}^*)_{\alpha} \nabla \partial_{\beta} f \times \nabla \partial_{\gamma} f \\ &= -\frac{i}{2} \varepsilon^{\alpha\beta\gamma} \langle L_{\alpha} \rangle \nabla \partial_{\beta} f \times \nabla \partial_{\gamma} f, \end{aligned} \quad (13)$$

where Eq. (11) has been adopted in the second line. Clearly, this is proportional to the components of OAM in the initial state. The remaining ‘‘form factor’’  $\nabla \partial_{\beta} f \times \nabla \partial_{\gamma} f$  depends on  $\mathbf{k}_F$ , which in turn depends on the incoming photon energy. Both  $\langle \mathbf{L} \rangle$  and the form factors can be obtained by faithful LDA calculations of the wave functions. Analytically, choosing  $f(r) \sim e^{-r/a}$ , for instance, yields  $f(k_F) = 1/(1+k_F^2 a^2)^2$  and the form factors can be worked out.

Next we turn to the case of degenerate  $d$ -orbital bands. Now  $g_\sigma = (\mathbf{m}_\sigma \cdot \mathbf{D})f$  involves the inner product between the five-dimensional coefficient vector  $\mathbf{m}_\sigma$  and the corresponding differential operators  $D_\alpha$  matching the given orbital basis. Examples are  $D_{xy} = \partial_x \partial_y$ ,  $D_{3z^2-r^2} = (2\partial_z^2 - \partial_x^2 - \partial_y^2)/2\sqrt{3}$ , etc. Although the dichroism formula (12) still applies, we are no longer able to transform its numerator to a simple form like Eq. (13). Recall that in realistic ARPES experiment the incident photons carry energies of several tens of eV, delivering however at most an eV of energy to the occupied electrons[7]. After subtracting what amounts to the surface potential energy barrier, there is still a lot of energy imparted to the final photo-electron, whose energy is typically in excess of 10 eV. Due to in-plane momentum conservation, the in-plane component of photo-electron momentum can carry only a small fraction of this energy, which means most of the kinetic energy is contained in the  $z$ -component,  $(k_{F,z})^2/2m$ . As a result, the typical situation in ARPES experiment is the one in which  $k_{F,z}$  dominates over the planar components, and  $k_{F,z}a$  is rather larger than unity,

$a$  being the radius of the orbital wave function.

In computing  $g_\sigma = (\mathbf{m}_\sigma \cdot \mathbf{D})f$ , therefore, the orbitals containing at least one power of  $z$  will be dominant over those that contain none, due to extra powers of  $k_F^z a$  produced by the differentiation. The reasoning reduces the number of relevant orbitals from five to three, i.e.  $d_{zx}$ ,  $d_{yz}$ , and  $d_{3z^2-r^2}$ . This is irrespective of particular crystal field symmetries of the  $d$ -orbitals and is rather dictated by the experimental conditions of ARPES. We also introduce the ‘‘partial OAM’’ obtained by assuming only the three, labeled  $1 \equiv zx$ ,  $2 \equiv yz$ , and  $3 \equiv 3z^2 - r^2$ , out of the five  $d$ -orbitals contribute to the wave function:  $\langle L_x \rangle' = \sqrt{3}i \sum_\sigma (m_{2,\sigma} m_{3,\sigma}^* - m_{2,\sigma}^* m_{3,\sigma})$ ,  $\langle L_y \rangle' = \sqrt{3}i \sum_\sigma (m_{3,\sigma} m_{1,\sigma}^* - m_{3,\sigma}^* m_{1,\sigma})$ ,  $\langle L_z \rangle' = i \sum_\sigma (m_{1,\sigma} m_{2,\sigma}^* - m_{1,\sigma}^* m_{2,\sigma})$ . The prime is a reminder that contributions average OAM from  $d_{xy}$  and  $d_{x^2-y^2}$  are missing. Following the same calculation procedure as in the  $p$ -orbital case, we find the CD formula for  $d$ -orbitals valid for  $k_{F,z}a \gg 1$ ,

$$D_d(\mathbf{k}) = \frac{\hat{k}_{\text{ph}} \cdot (2\langle L_x \rangle' \hat{x} + 2\langle L_y \rangle' \hat{y} - \langle L_z \rangle' \hat{z})}{\sum_\sigma [A_x m_{1,\sigma} + A_y m_{2,\sigma} - 2\sqrt{3}A_z m_{3,\sigma}] [(A_x)^* m_{1,\sigma}^* + (A_y)^* m_{2,\sigma}^* - 2\sqrt{3}(A_z)^* m_{3,\sigma}^*] + (\mathbf{A} \leftrightarrow \mathbf{A}^*)}. \quad (14)$$

The OAM shown in the numerator refers to those in partial OAM. Again, non-trivial CD-ARPES signal is predicated on the existence of OAM. In the same limit,  $k_{F,z}a \gg 1$ , the  $p$ -orbital formula simplifies to

$$D_p(\mathbf{k}) = \frac{5\hat{k}_{\text{ph}} \cdot \langle \mathbf{L} \rangle - 6(\hat{k}_{\text{ph}} \cdot \hat{k}_F)(\hat{k}_F \cdot \langle \mathbf{L} \rangle)}{\sum_\sigma [6(\hat{k}_F \cdot \mathbf{A})(\hat{k}_F \cdot \mathbf{m}_\sigma) - (\mathbf{m}_\sigma \cdot \mathbf{A})][6(\hat{k}_F \cdot \mathbf{A}^*)(\hat{k}_F \cdot \mathbf{m}_\sigma^*) - (\mathbf{m}_\sigma^* \cdot \mathbf{A}^*)] + (\mathbf{A} \leftrightarrow \mathbf{A}^*)}. \quad (15)$$

The case of  $t_{2g}$ -bands involving the three orbitals,  $yz \equiv 1$ ,  $zx \equiv 2$ , and  $xy \equiv 3$  can be considered as well. The factor  $\sum_\sigma \nabla g_\sigma \times \nabla g_\sigma^*$  in Eq. (12) becomes

$$\frac{1}{2} \varepsilon^{\alpha\beta\gamma} \left( \sum_\sigma \mathbf{m}_\sigma \times \mathbf{m}_\sigma^* \right)_\alpha \nabla D_\beta f \times \nabla D_\gamma f, \quad (16)$$

where  $\mathbf{D} = (D_{yz}, D_{zx}, D_{xy})$ . As in the  $p$ -orbital case, we obtain a simple relation for the OAM average of the given Bloch state in the  $t_{2g}$ -band:  $\langle \mathbf{L} \rangle = -i \sum_\sigma \mathbf{m}_\sigma \times \mathbf{m}_\sigma^*$ . (Note the opposite sign compared to the  $p$ -orbital result in Eq. (11).) Again, non-trivial OAM is responsible for NCD for  $t_{2g}$ -bands. The actual task of evaluating the form factors leads to cumbersome expressions. For practical applications, it is better to evaluate them numerically using LDA-obtained wave functions.

The OAM of the Bi bands shown in Fig. 1(a) is used to obtain  $D(\mathbf{k})$  according to Eqs. (12) and (13). Exponential function  $f(r) \sim e^{-r/a}$  with the radius  $a = 1.6\text{\AA}$  was

used to evaluate the form factors. Figure 1(b)-(d) shows  $D(\mathbf{k})$  overlaid with local OAM when  $\mathbf{k}_F = 2.27\text{\AA}^{-1}$ . The next set of figures in (e) and (f) is obtained with  $\mathbf{k}_F = 0\text{\AA}^{-1}$  for  $E_2$  and  $E_3$  bands. Incident photon direction is chosen  $\hat{k}_{\text{ph}} = (\cos 60^\circ, 0, -\sin 60^\circ)$  in both sets. The photon energy dependence of the NCD is obvious by comparing Fig. 1(c) with (e). LDA calculation for light-element  $d$ -orbital bands are under way and will be reported elsewhere, along with some experimental results[9]. We comment that a potential modification of the NCD formula may be necessary for heavy elements due to significant spin-orbit interaction in the Hamiltonian and the consequent modification of the current (momentum) operator coupling to  $\mathbf{A}$ [10]. Our present results are, however, free from such complications as we exclusively focus on spin-degenerate band structures. Non-trivial OAM and NCD features are only due to the degenerate multiple-orbital nature of the eigenstates.

This work is supported by Mid-career Researcher Pro-

gram No. 2011-0015631 (JHH).

---

\* Electronic address: [hanjh@skku.edu](mailto:hanjh@skku.edu)

- [1] Y. A. Bychkov and E. I. Rashba, JETP Lett. **39**, 78 (1984).
- [2] G. Bihlmayer, Yu. M. Koroteev, P. M. Echenique, E. V. Chulkov and S. Blügel, Surf. Sci. **600**, 3888 (2006).
- [3] J. H. Dil, J. Phys. Condens. Matter **21**, 403001 (2009).
- [4] A. Kimura *et al.* Phys. Rev. Lett. **105**, 076804 (2010).
- [5] L. Petersen and P. Hedegård, Surf. Sci. **459**, 49 (2000).
- [6] P. Olbrich, S. A. Tarasenko, C. Reitmaier, J. Karch, D. Plohmman, Z. D. Kvon, and S. D. Ganichev, Phys. Rev. B **79**, 121302(R) (2009).
- [7] A. Damascelli, Z. Hussain and Z.-X. Shen, Rev. Mod. Phys. **75**, 473 (2003).
- [8] Y. Liu and R. E. Allen, Phys. Rev. B **52**, 1566 (1995).
- [9] In preparation.
- [10] Y. H. Wang, D. Hsieh, D. Pilon, L. Fu, D. R. Gardner, Y. S. Lee, and N. Gedik, Phys. Rev. Lett. **107**, 207602 (2011).